IOPscience iopscience.iop.org

Home Search Collections Journals About Contact us My IOPscience

Non-linear conductance of a saddle-point constriction

This article has been downloaded from IOPscience. Please scroll down to see the full text article.

1992 J. Phys.: Condens. Matter 4 1323

(http://iopscience.iop.org/0953-8984/4/5/012)

View the table of contents for this issue, or go to the journal homepage for more

Download details:
IP Address: 171.66.16.159
The article was downloaded on 12/05/2010 at 11:13

Please note that terms and conditions apply.

J. Phys.: Condens. Matter 4 (1992) 1323–1333. Printed in the UK

Non-linear conductance of a saddle-point constriction

L Martín-Moreno, J T Nicholls, N K Patel and M Pepper
Cavendish Laboratory, Madingley Road, Cambridge CB3 0HE, UK

Received 13 November 1991

Abstract. We present calculations of the differential conductance, G, of a constriction, defined by a saddle-point potential in a two-dimensional electron gas, in the non-linear regime of transport as a function of Fermi energy, source–drain voltage and magnetic field. The manner in which the potential is dropped along the device is considered phenomenologically. The dependence of G on the parameters that define the potential drop is investigated, extending the model proposed by Glazman and Khaetskii. A method for measuring the sub-band energies and spin-splitting energies in a bottle-neck of the constriction is also proposed. Finally, a comparison between experimental data and theoretical calculations is presented.

1. Introduction

A few years ago, the conductance of a quantum point contact (QPC) defined by applying a negative voltage to a split-gate over the two-dimensional electron gas (2DEG) formed at a GaAs–AlGaAs heterojunction [1,2] was found to be quantized [3,4] in multiples of $2e^2/h$. The constriction was short enough for the electrons to cross it ballistically. Although most of the experimental and theoretical studies on such devices have concentrated on the linear regime of transport, [5] the non-linear regime has also received some attention, and can be divided into two limits: (i) when the potential difference due to the source–drain voltage eV_{sd} is larger than the Fermi energy E_F, and (ii) when eV_{sd}, is comparable to the sub-band energy spacings ΔE. For the case when $eV_{sd} > E_F$ it is predicted [6] that as V_{sd} is increased a QPC should show negative differential resistance, due to a saturation of the number of carriers and a decrease of the transmission probabilities through the constriction. Hints of instabilities in the conductance associated with negative differential resistance have been observed in some experiments [7], but not in others [8,9]. For the case when $eV_{sd} \approx \Delta E$, the theoretical calculations are more complicated than those in the linear response regime because the current and the electrostatic potential have to be calculated self-consistently for each value of the source–drain voltage. Self-consistent calculations are difficult even for a simple 2D system and, in the simulation of real devices, there is the additional complication of the presence of gates.

To date, all theoretical studies on the non-linear differential conductance of QPCs have made assumptions about how the potential difference due to the source–drain voltage is dropped along the device. Glazman and Khaetskii (GK) assumed [10] that half of the source–drain voltage is dropped between the contacts and the 'bottle-neck' of the constriction. For constrictions whose width varies very slowly (adiabatic constrictions), GK predicted [10] new plateaux in the differential conductance for $V_{sd} \neq 0$

 © 1992 IOP Publishing Ltd

(called 'half-plateaux'), appearing midway between the plateaux observed at $V_{sd} = 0$. If the source–drain voltage is dropped linearly along the constriction, calculations of the differential conductance $G = \mathrm{d}I/\mathrm{d}V_{sd}$ of a constriction defined by abrupt changes in the geometry (the wide–narrow–wide model) do not show half-plateaux [11, 12]. Instead, the calculations [11, 12] show a smearing of the conductance plateaux and a disappearance of the structure on top of the plateaux (length resonances) that is characteristic of these wide–narrow–wide models [13, 14]. Bagwell and Orlando [15], while addressing the importance of self-consistency, did not attempt to include it in their calculation of the non-linear conductance of a quantum-point contact and therefore found a smearing of the zero-bias plateaux but no half-plateaux.

Kouwenhoven *et al* [8] studied experimentally the I–V_{sd} characteristics of a quantum-point contact with a small number of occupied conducting sub-bands. Half-plateaux were not observed in their device, but the onset of non-linearities in the I–V_{sd} curves could be explained by a model similar to that proposed by GK. Kouwenhoven *et al* [8] estimated that half of the source–drain voltage is dropped between the source and the bottle-neck of the constriction when the differential conductance is over $2e^2/h$, but only 20% is dropped when G is smaller than $2e^2/h$, implying that the measured fraction of the voltage dropped at the narrowest point of the device is not a universal quantity. Experiments by Patel *et al* [9] clearly showed the half-plateaux in the differential conductance, appearing approximately midway between the integer plateaux for $G \geqslant 2e^2/h$. For $G < 2e^2/h$, no half-plateau was found; instead, structure was observed [9] at $G \approx 0.2(2e^2/h)$. Although the appearance of half-plateaux could be caused by spin splitting induced by the electric field [16], this possibility has been ruled out by recent experiments [17, 18] that show a splitting of the half-plateaux under an applied magnetic field, proving that the voltage-induced half-plateaux originate from spin-degenerate sub-bands.

For special values of the gate voltage the non-linear characteristics of a quantum point contact have been used [8,9] to obtain the sub-band energy spacings in the bottle-neck of the constriction. In such experiments it is not necessary to scale the gate voltage in terms of the sub-band energy, in contrast to earlier, less direct methods, where the depopulation of the sub-bands in a perpendicular magnetic field was fitted to theoretical models [19, 20]. Recently, a method for obtaining the sub-band spacings for arbitrary gate voltage has been proposed [21, 22]. In this method, one exploits the relation of the sub-band spacing to the length in source–drain voltage of the half-plateaux, that is, to the source–drain voltages needed, firstly, to produce a half-plateau and, secondly, to return from a half-plateau to an integer plateau.

The rest of this paper is organized as follows. In section 2, previous theoretical studies are briefly reviewed and extended by considering more general ways in which the source–drain voltage is dropped across a split-gate device. Calculations of the differential conductance for a saddle-point constriction are presented in section 3, and the theoretical calculations and the experimental data are compared in section 4. Conclusions are given in section 5.

2. Adiabatic constriction

Before discussing the differential conductance as a function of source–drain voltage for the saddle-point constriction, it is convenient to consider first a simplified model [10, 23] that shows clearly the effects of an applied source–drain voltage V_{sd}. In this model the constriction in the 2DEG is defined by hard walls, with a width that varies very slowly (adiabatically). In adiabatic constrictions the intermode scattering can be neglected [23], and the transport through such a system is equivalent to a set of strictly one-dimensional (1D) problems of transport through a barrier, one for each incident mode. At $V_{sd} = 0$, the maximum of the nth 1D barrier E_n (the barrier for the electrons coming from the nth transverse mode in the wide region that acts as a source reservoir) is the nth energy eigenvalue of the confining potential in the bottle-neck of the constriction. For finite V_{sd}, the maximum energy of the nth 1D barrier depends on how the applied source–drain voltage is dropped along the device, and is labelled as $E_n(V_{sd})$. Because the barriers are smooth, the transmission probability through the nth 1D barrier is well approximated [10,23] by the classical expression $T_n(E, V_{sd}) = \Theta(E - E_n(V_{sd}))$, where $\Theta(x) = 1$ for $x > 0$ and $\Theta(x) = 0$ for $x < 0$.

Assuming that transport is still ballistic for finite V_{sd}, the zero-temperature Landauer formula [5,24] for the current in the linear response regime can be extended to finite V_{sd}, and is given by

$$I(V_{sd}) = \frac{2e}{h} \sum_n \int_{\min(E_F - eV_{sd}, 0)}^{E_F} T_n(E, V_{sd})\, \mathrm{d}E. \tag{1}$$

For the cases considered in this paper, $eV_{sd} < E_F$, and the differential conductance G is given by

$$G = \frac{\mathrm{d}I}{\mathrm{d}V_{sd}} = \frac{2e^2}{h} \sum_n \left[\left(1 + \frac{\mathrm{d}E_n(V_{sd})}{\mathrm{d}(eV_{sd})}\right) \Theta(E_F - eV_{sd} - E_n(V_{sd})) - \frac{\mathrm{d}E_n(V_{sd})}{\mathrm{d}(eV_{sd})} \Theta(E_F - E_n(V_{sd})) \right]. \tag{2}$$

If the voltage dropped at the bottle-neck of the constriction is linear in V_{sd}, the $E_n(V_{sd}) = E_n - \beta e V_{sd}$, and (2) predicts that new plateaux will be introduced by V_{sd}. Equation (2) then simplifies to

$$G = (2e^2/h)\{\beta N_+ + (1 - \beta) N_-\} \tag{3}$$

where N_+ is the sub-band number such that $E_{N_+} < E_F + \beta e V_{sd} < E_{N_+ + 1}$, and N_- is the sub-band number such that $E_{N_-} < E_F - (1 - \beta) e V_{sd} < E_{N_- + 1}$. Equation (3) predicts new plateaux in the differential conductance at values of $G = (N + \beta)2e^2/h, (N + 2\beta)2e^2/h, (N + 3\beta)2e^2/h, \ldots$, where N is an integer, depending on whether the numbers of conducting sub-bands in the forward and backward directions differ by 1,2,3 and so-on, respectively.

The physical origin of the half-plateaux can be more clearly seen if we use an energy reference frame in which the sub-band energies E_n remain constant as a function of V_{sd}. In this reference frame, when a voltage difference is applied, the electrochemical potential at the source reservoir is $\mu_s = E_F + \beta e V_{sd}$, and the electrochemical potential at the drain reservoir is $\mu_d = E_F - (1 - \beta) e V_{sd}$. The total current, I, is due to electrons in the energy interval between μ_d and μ_s, whereas the differential conductance is related to electrons with energies close to the source and drain electrochemical potentials. Therefore, the differential conductance at finite V_{sd}

is a weighted average of two zero-V_{sd} conductances (see (3)), one for a Fermi energy of $E_F + \beta e V_{sd}$, and the other for a Fermi energy of $E_F - (1-\beta)eV_{sd}$. When the number of occupied sub-bands is different for these two 'Fermi energies', the average differential conductance is not necessarily an integer multiple of $2e^2/h$.

GK calculated [10] that, in adiabatic constrictions, $\beta \approx \frac{1}{2}$ when there is a large number of occupied sub-bands. Experimentally it has been found [8,9] that $\beta \approx \frac{1}{2}$ even for a small number of occupied conducting sub-bands, except when only the forward direction is populated (when $G < 2e^2/h$). However, a consideration of more general dependences of the voltage dropped at the bottle-neck of the constriction is of interest for the case of highly asymmetric constrictions.

From the $G(V_{sd})$ traces at fixed Fermi energy it is possible to obtain the sub-band energy spacings. Consider the Fermi energy to be somewhere between E_N and E_{N+1}. If the source–drain voltage is increased, the conductance remains on the same plateau until either the electrochemical potential at the source reservoir μ_s becomes equal to $E_{N+1}(V_{sd})$, or the electrochemical potential at the drain reservoir μ_d becomes equal to $E_N(V_{sd})$. At such a point the differential conductance switches to a value $(N+\beta)2e^2/h$ or $(N-(1-\beta))2e^2/h$, respectively. For the case where the differential conductance switches to $(N+\beta)2e^2/h$, when $\mu_s = E_{N+1}(V_{sd})$, we label the source–drain voltage at which this change occurs as V_1. The value of V_1 can be found as a maximum in dG/dV_{sd}, at which

$$E_F + \beta e V_1 = E_{N+1}. \tag{4}$$

On increasing the source–drain voltage further, dG/dV_{sd} should reach a minimum at a voltage V_2 given by

$$E_F - (1-\beta)eV_2 = E_N. \tag{5}$$

Subtracting (5) from (4), we obtain the sub-band energy spacing

$$E_{N+1} - E_N = e[V_2(1-\beta) + \beta V_1]. \tag{6}$$

For different combinations of maxima and minima we obtain (defining V_1 as the source–drain voltage of the first extremum in dG/dV_{sd}, and V_2 as the second extremum),

$$E_{N+1} - E_N = e[V_1(1-\beta) + \beta V_2] \tag{7}$$

if V_1 corresponds to a minimum and V_2 to a maximum;

$$E_{N+2} - E_{N+1} = \beta e(V_2 - V_1) \tag{8}$$

if V_1 corresponds to a maximum and V_2 to a maximum; and

$$E_N - E_{N-1} = (1-\beta)e(V_2 - V_1) \tag{9}$$

if V_1 corresponds to a minimum and V_2 to a minimum.

If more than two extrema occur in the dG/dV_{sd} curves as a function of V_{sd}, additional sub-band spacings can easily be determined. If $\beta = \frac{1}{2}$, (6) and (7) reduce to the result derived by Zagoskin [21].

In the adiabatic model we require that $eV_{sd} < E_F$ and that the transport remains ballistic for the range of V_{sd} considered; however we have not specified the nature of the 1D sub-bands in the bottle-neck. In a high magnetic field the energies E_n are the minima of the spin-split 1D sub-bands and the method described above can be used to measure the Zeeman energy, $2g\mu_B SB$, and hence the g-factor in the bottle-neck of the constriction can be measured [18].

3. The saddle-point potential

A model that includes tunnelling and quantum reflection of the electrons at the constriction is needed in order to explain more quantitatively the experimental data. The saddle-point potential [25] is such a model, and can be regarded as neglecting all but the linear and quadratic terms in the Taylor expansion of the electrostatic potential near the bottle-neck of the constriction. If the transport is globally adiabatic [26], it is the bottle-neck that determines the transport properties of the QPC.

We consider a constriction formed by a saddle-point potential in two dimensions. We assume that, as a function of V_{sd}, the shape of the saddle-point potential does not change, but the electrostatic potential energy in the saddle point $U_0(V_{sd})$ is a function of V_{sd}. Including the Zeeman energy, the potential energy close to the bottle-neck of the constriction is

$$U(x,y) = U_0(V_{sd}) + \tfrac{1}{2}m^*\omega_y^2 y^2 - \tfrac{1}{2}m^*\omega_x^2 x^2 \pm g\mu_B SB \tag{10}$$

where m^* is the electron effective mass, g is the Landé g-factor (which, for simplicity, we assume to be isotropic), $S = \frac{1}{2}$ is the electron spin, B is the magnetic field, ω_y and ω_x are parameters that define the shape of the saddle, and x and y are the coordinates in the plane.

The transmission probability through this potential can be calculated analytically, even in the presence of a perpendicular magnetic field [27]. The current $I(V_{sd})$ and the differential conductance $G(V_{sd})$ can be calculated using (1) and (2), and G is given by

$$G = \frac{e^2}{h}\sum_{n=1}^{\infty}\sum_{S=\pm 1/2} g_{nS} \tag{11}$$

where

$$\begin{aligned} g_{nS} = {} & \big(1 + \mathrm{d}U_0(V_{sd})/\mathrm{d}(eV_{sd})\big) \\ & \times \exp\big[(E_{Fn} + g\mu_B SB)/E_1\big]\big\{1 + \exp[(E_{Fn} + g\mu_B SB)/E_1]\big\}^{-1} \\ & - \big(\mathrm{d}U_0(V_{sd})/\mathrm{d}(eV_{sd})\big)\exp\big[(E_{Fn} - eV_{sd} + g\mu_B SB)/E_1\big] \\ & \times \big\{1 + \exp\big[(E_{Fn} - eV_{sd} + g\mu_B SB)/E_1\big]\big\}^{-1} \end{aligned} \tag{12}$$

$$E_{Fn} = E_F - U_0(V_{sd}) - (n + \tfrac{1}{2})E_2 \tag{13}$$

$$E_1 = (\hbar/2\pi\sqrt{2})\big\{\big[(\omega_c^2 + \omega_y^2 - \omega_x^2)^2 + 4\omega_x^2\omega_y^2\big]^{1/2} - (\omega_c^2 + \omega_y^2 - \omega_x^2)\big\}^{1/2} \tag{14}$$

$$E_2 = (\hbar/\sqrt{2})\big\{\big[(\omega_c^2 + \omega_y^2 - \omega_x^2)^2 + 4\omega_x^2\omega_y^2\big]^{1/2} + (\omega_c^2 + \omega_y^2 - \omega_x^2)\big\}^{1/2} \tag{15}$$

$$\omega_c = eB_\perp/m^* \tag{16}$$

and $B_\perp$ is the component of the magnetic field perpendicular to the 2DEG.

We shall calculate the differential conductance for different values of the various parameters. All the calculations presented in this paper use the ratio $\omega_y/\omega_x = 2$,

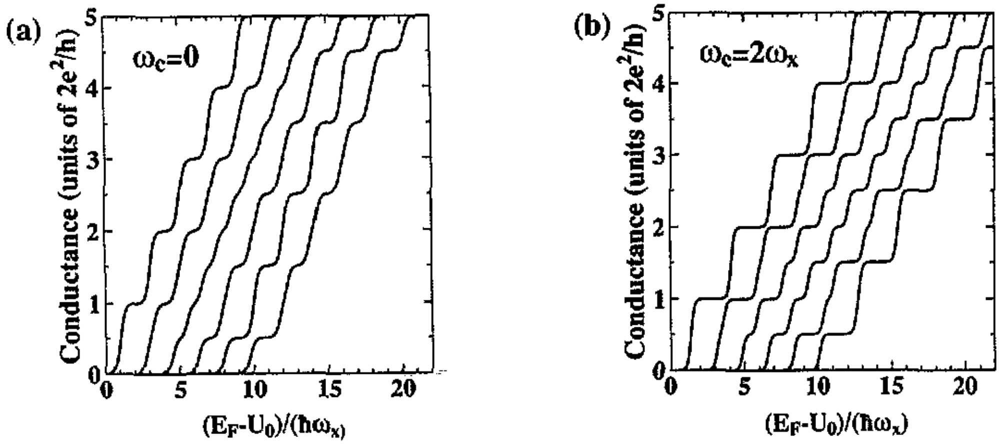

Figure 1. (a) The differential conductance versus the Fermi energy $E_F - U_0$ at zero magnetic field for a 2D saddle-point constriction, with DC source–drain voltages varying from 0 (left trace) to $2.5\hbar\omega_x$ (right trace) in increments of $0.5\hbar\omega_x$. The parameter ω_y/ω_x is taken to be 2, and the potential energy in the saddle point is assumed to depend linearly on the source-drain voltage as $U_0(V_{sd}) = U_0 - 1/2eV_{sd}$. For clarity, successive traces are shifted laterally by $2\hbar\omega_x$. (b) As in (a), but in the presence of a perpendicular magnetic field corresponding to a cyclotron frequency $\omega_c = 2\omega_x$. The spin-splitting energy is neglected.

a value that best agrees with the shape of the $G(V_g)$ traces of good-quality devices [22].

To produce half-plateaux, we shall consider first the case $U_0(V_{sd}) = U_0 - 1/2eV_{sd}$, where U_0 is the electrostatic potential in the saddle point at $V_{sd} = 0$. Figure 1(a) shows the differential conductance as a function of the Fermi energy for different values of V_{sd}, from $V_{sd} = 0$ (left trace) to $V_{sd} = 2.5\hbar\omega_x$ (right trace), in source–drain voltage increments of $0.5\hbar\omega_x$. For clarity, successive traces have been shifted laterally by $2\hbar\omega_x$. The left trace ($V_{sd} = 0$) shows the usual conductance plateaux at integer multiples of $2e^2/h$. As V_{sd} is increased the integer plateaux become shorter while new structure develops in the conductance at half-integer values of $2e^2/h$; these are the half-plateaux. In figure 1(a), the integer plateaux disappear approximately when the half-plateaux appear, as found experimentally [9,22]. This is a consequence of the range of parameters considered: if δE is the energy range over which the transmission probability varies from 0 to 1, and ΔE is the energy difference between the bottoms of consecutive sub-bands (in this model ΔE does not depend on the sub-band index), then integer plateaux are expected when $\Delta E - \delta E > eV_{sd}$, and half-plateaux are expected when $\delta E < eV_{sd}$. In zero magnetic field, where $\Delta E = \hbar\omega_y$ and $\delta E \approx \hbar\omega_x$, the calculations in figure 1(a) show that integer plateaux and half-plateaux do not coexist for $\omega_y/\omega_x = 2$. However, if $B_\perp \neq 0$, the sub-band energy spacing increases, the transmission probability versus energy becomes sharper [25], (that is $\Delta E > \hbar\omega_y$ and $\delta E < \hbar\omega_x$), and the curves in figure 1(b) show that integer plateaux and half-plateaux can coexist for some range of source–drain voltages.

Figure 2 shows the differential conductance, G, plotted as a function of V_{sd}, for different values of the Fermi energy $E_F - U_0$. For some ranges of E_F, the conductance remains approximately constant, and if G were plotted versus $E_F - U_0$

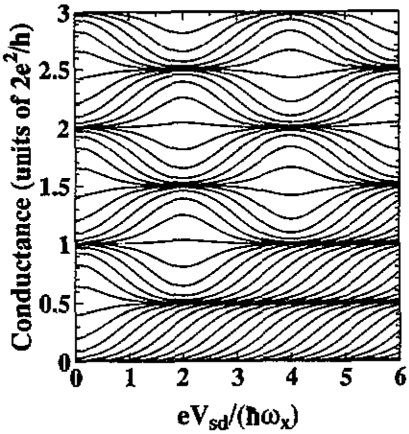

Figure 2. The differential conductance versus source–drain voltage V_{sd} (in units of $\hbar\omega_x$) for a 2D saddle-point constriction. Each trace is calculated for a fixed value of $E_F - U_0$ that differs by $(5/32)\hbar\omega_x$ between consecutive traces. The values $\omega_y/\omega_x = 2$, $U_0(V_{sd}) = U_0 - \frac{1}{2}eV_{sd}$ and $B = 0$ were used in the calculation.

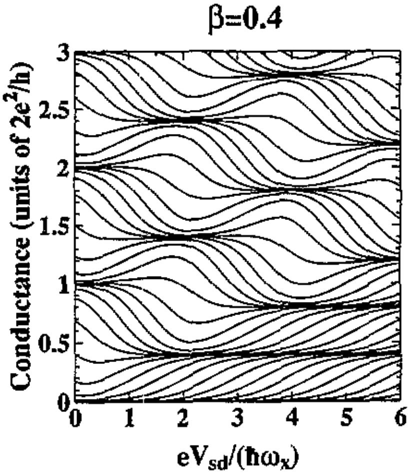

Figure 3. The same parameters as in figure 2, except for $U_0(V_{sd}) = U_0 - 0.4eV_{sd}$.

curves similar to those in figure 1(*a*) would be obtained. Figure 2 shows clearly the conductance oscillating between integer and half-integer multiples of $2e^2/h$, as the electrochemical potentials on the left and right reservoirs align with the sub-band energies, as predicted in the previous section for $\beta = \frac{1}{2}$. If a different confining potential were considered, it would be necessary to rescale the V_{sd} axis, but otherwise the results would be qualitatively similar to those shown in figure 2.

The effect of an asymmetric voltage drop on the differential conductance of a QPC as a function of source–drain voltage is shown in figure 3, where $\beta = 0.4$, and all other parameters are the same as those used in figure 2. When the source–drain voltage is of the order of the sub-band energy spacing $eV_{sd} \approx \hbar\omega_y = 2\hbar\omega_x$, figure 3 shows plateaux appearing at $G/(2e^2/h) = 0.4, 1.4, 2.4, \ldots$ and plateaux at $G/(2e^2/h) = 0.4, 0.8, 1.8, 2.8\ldots$ when $V_{sd} \approx 2\hbar\omega_y = 4\hbar\omega_x$, in agreement with (3).

A magnetic field parallel to the 2DEG shifts the bottom of the energy sub-bands by the Zeeman term $\pm g\mu_B SB$. The lifting of the spin degeneracy gives rise to conductance plateaux at integer multiples of e^2/h. These extra plateaux are independent of the V_{sd}-induced half-plateaux and, therefore, in a high parallel magnetic field and in high V_{sd} 'quarter-plateaux' are observed at multiples of $e^2/2h$. Figure 4(*a*) shows the effect of a parallel magnetic field on the conductance versus V_{sd} curves, for a value of $2g\mu_B SB = 0.8\hbar\omega_x$. A value of $\beta = \frac{1}{2}$ was used, as in figures 1 and 2. Although the traces in an applied parallel magnetic field (see figure 4(*a*)) are qualitatively different to the traces for zero magnetic field (see figure 2), the quarter-plateaux are not well resolved in figure 4(*a*). To make the quarter-plateaux more distinct we can use either a larger value of the parallel magnetic field, or a tilted magnetic field. Figure 4(*b*) shows the results for the same set of parameters as in figure 4(*a*), using a tilted mag-

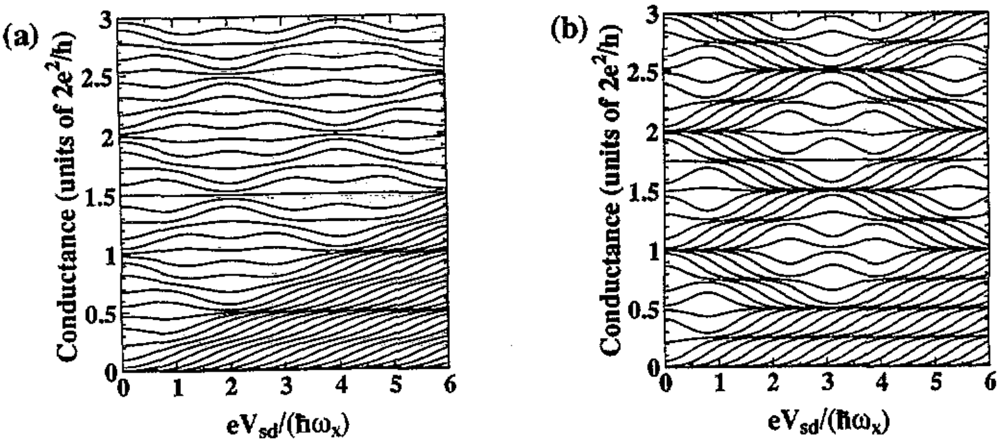

Figure 4. (*a*) The differential conductance versus source–drain voltage for a 2D saddle-point constriction. Each trace is calculated for a fixed value of $E_F - U_0$ that differs by $(5/32)\hbar\omega_x$ between consecutive traces. The values $\omega_y/\omega_x = 2$ and $U_0(V_{sd}) = U_0 - \frac{1}{2}eV_{sd}$ are the same as those used in figure 2, except that here the Zeeman energy is taken to be $2g\mu_B SB = 0.8\hbar\omega_x$. (*b*) As in (*a*) but with a tilted magnetic field such that the cyclotron frequency $\omega_c = 2\omega_x$.

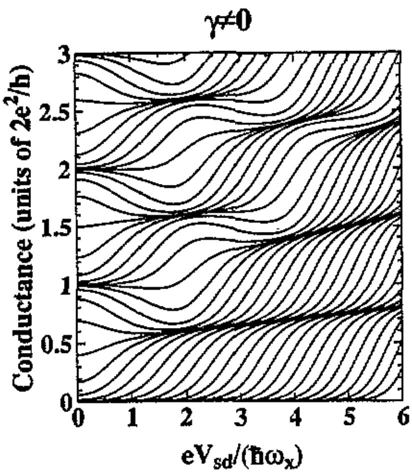

Figure 5. The differential conductance versus source–drain voltage for a 2D saddle-point constriction, showing the effect of a non-linear drop of the potential between the source and the bottle-neck of the constriction. For the case shown $U_0(V_{sd}) = U_0 - \frac{1}{2}eV_{sd} + \gamma eV_{sd}^2/2$. Each trace is calculated for a fixed value of $E_F - U_0$ that differs by $(5/32)\hbar\omega_x$ between consecutive traces. The values $\omega_y/\omega_x = 2$, $\gamma = 0.05e/\hbar\omega_x$ and $B = 0$ were used in the calculation.

netic field with a perpendicular component corresponding to a cyclotron frequency of $\omega_c = 2\omega_x$. Due to the increased sharpness of the transmission probability caused by $B_\perp$, quarter-plateaux can be clearly seen for finite V_{sd} at conductance values of $G/(2e^2/h) = 1.25$, 1.75, 2.25, and 2.75.

The effect of a non-linear voltage drop between the source and the bottle-neck of the constriction can be modelled by adding a quadratic term to the dependence of the electrostatic potential at the bottle-neck on the source–drain voltage. The potential then becomes $U_0(V_{sd}) = U_0 - \beta e V_{sd} + \gamma e V_{sd}^2/2$. Figure 5 shows calculations of $G(V_{sd})$ with the same parameters as figure 2, and including the extra term $\gamma = 0.05e/\hbar\omega_x$. The half-plateaux now drift to higher values of conductance (or lower values if γ is negative) as a function of V_{sd}. If γ were larger or, more generally, if the departures from linearity of $U_0(V_{sd})$ were significant, then the half-plateaux would not appear.

4. Comparison between theory and experiment

In this section we present the comparison between the measured $G(V_{sd})$ for several values of the gate voltage, and the calculated $G(V_{sd})$ of a saddle-point constriction for several values of the Fermi energy $E_F - U_0$.

Applying a negative voltage to the split gate of a QPC changes both the average electrostatic potential near the constriction (the term U_0 in (10)) and the width and length of the constriction, represented by ω_y and ω_x, respectively, (see (10)). In order to compare experiment and theory, it is necessary to know the dependence of the potential at the bottle-neck on the gate voltage. We shall assume that the change of the gate voltage V_g is linearly related to the change in the electrostatic potential at the saddle point U_0. This approximation should be valid for small variations of gate voltage.

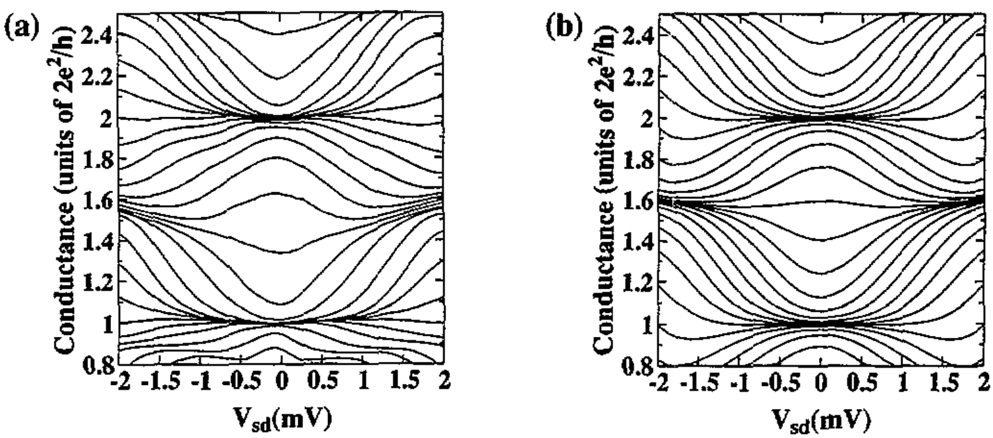

Figure 6. (*a*) The experimental differential conductance as a function of source–drain voltage for different gate voltages at $B = 0$. (*b*) The calculated differential conductance as a function of source–drain voltage for a saddle-point constriction, using $B = 0$, $U_0(V_{sd}) = U_0 - \frac{1}{2}eV_{sd} + 0.025(eV_{sd})^2$, $\hbar\omega_y = 2$ meV, and $\hbar\omega_x = 1$ meV. Each trace is calculated for fixed value of $E_F - U_0$, which differs by 0.125 meV between consecutive traces.

Figure 6 shows the comparison between the experimental differential conductance data taken at $T = 40$ mK for a standard split-gate device, with characteristics presented elsewhere [22], and the theoretical curves obtained from (11)–(16). From the shape of the experimental traces of $G(V_g)$ taken at $V_{sd} = 0$ we obtain [22] the value of the ratio $\omega_y/\omega_x = 2$. From the bunching of the experimental curves in figure 6(*a*) at $V_{sd} = \pm 2$ mV about a conductance value of $G \approx 1.5(2e^2/h)$, we obtain $2\hbar\omega_y = 2$ meV and $\beta = \frac{1}{2}$. The small overall positive slope of the experimental $G(V_{sd})$ could be due to a non-linear dependence of the potential, $U_0(V_{sd})$, on the source–drain voltage, that can be modelled by a small and positive γ (see figure 5). For the calculations shown in figure 6(*b*) we have used a value $\gamma/e = 0.05$ meV^{-1}, giving a potential energy at the saddle point $U_0(V_{sd}) = U_0 - 0.5eV_{sd} + 0.025(eV_{sd})^2$, where V_{sd} is expressed in mV. For the range of conductances shown, there is good agreement between the experimental results and the calculations, in support of the model in which approximately half the potential is dropped between the contacts and the bottle-neck of the constriction.

The comparison between experiment and theory for high magnetic fields is of interest because the g-factors of the quasi-1D electron gas can be extracted, and has been presented elsewhere [17, 18].

It is important to note that there are two regimes where the experimental $G(V_{sd})$ data cannot be explained by the GK model or the saddle-point potential model:

(i) when $V_{sd} > 4$ mV the conductance traces decrease smoothly [22], indicating a transition to the non-ballistic regime where the model discussed here is no longer applicable. In analogy with the experiments on metal point-contacts [28] structure observed in $I(V_{sd})$ for $V_{sd} > 4$ mV has been associated [29] with the phonon density of states.

(ii) For $G < 2e^2/h$, the experimental data shows structure [22] that is qualitatively different from the structure for $G > 2e^2/h$.

5. Conclusions

We have studied the non-linear differential conductance $G(V_{sd})$ of a system of independent electrons at zero temperature in a 2DEG, where the potential energy of the constriction is defined by the saddle-point model. We have presented results for G as a function of Fermi energy, source–drain voltage V_{sd}, parallel and perpendicular magnetic fields, and the way in which the potential is dropped across the device. When the potential at the bottle-neck of the constriction is linear in V_{sd}, additional quantization appears in the $G(E_F)$ curves when the source–drain voltage causes the number of conducting sub-bands in the forward and backward directions of transport to differ by one. The additional plateaux can be split further by a magnetic field, giving rise to quantization of the conductance in units of $e^2/2h$ (for devices in which half of the voltage V_{sd} is dropped between the source and the bottle-neck of the constriction). The use of tilted magnetic fields would help the experimental detection of these $e^2/2h$ conductance plateaux.

The method of measuring the sub-band energy spacings proposed by Zagoskin [21] has been extended to more general forms of voltage drops that may be relevant for highly asymmetric devices.

Finally, we have made a comparison between the experimental data and theoretical calculations of the conductance as a function of source–drain voltage V_{sd}. The good agreement obtained for $G > 2e^2/h$ shows that, for a quantum point contact device that is nominally symmetric, half of the voltage V_{sd} is dropped between the source and the bottle-neck of the constriction.

Acknowledgments

We would like to thank Dr D H Cobden for his comments on the manuscript. This work was supported by the SERC and by the EEC under the auspices of ESPRIT Basic Research Action, 3043, and the European Research Office of the US Army. LMM acknowledges support from Spain's Ministerio de Educación y Ciencia, and JTN acknowledges support from the Leverhulme Trust and the I Newton Trust.

References

[1] Thornton T J, Pepper M, Ahmed H, Andrews D and Davies G J 1986 *Phys. Rev. Lett.* **56** 1198
[2] Berggren K-F, Thornton T J, Pepper M, Ahmed H, Andrews D and Davies G J 1986 *Phys. Rev. Lett.* **57** 1769
[3] van Wees B J, van Houten H, Beenakker C W J, Williamson J G, Kouwenhoven L P, van der Marel D and Foxon C T 1988 *Phys. Rev. Lett.* **60** 848
[4] Wharam D A, Thornton T J, Newbury R, Pepper M, Ahmed H, Frost J E F, Hasko D G, Peacock D C, Ritchie D A and Jones G A C 1988 *J. Phys.: Condens. Matter* **21** L209
[5] Beenakker C W J and van Houten H 1990 *Solid State Physics* vol 44 (New York: Academic)
[6] Kelly M J 1989 *J. Phys.: Condens. Matter* **1** 7643
[7] Brown R J, Kelly M J, Pepper M, Ahmed H, Hasko D G, Peacock D C, Frost J E F, Ritchie D A and Jones G A C 1989 *J. Phys.: Condens. Matter* **1** 6285
[8] Kouwenhoven L P, van Wees B J, Harmans C J P M, Williamson J G, van Houten H, Beenakker C W J, Foxon C T and Harris J J 1989 *Phys. Rev.* B **39** 8040
[9] Patel N K, Martín-Moreno L, Pepper M, Newbury R, Frost J E F, Ritchie D A, Jones G A C, Janssen J T M B, Singleton J and Perenboom J A A J 1990 *J. Phys.: Condens. Matter* **2** 7247
[10] Glazman L I and Khaetskii A V 1989 *Europhys. Lett.* **9** 263
[11] Castaño E and Kirczenow G 1990 *Phys. Rev.* B **41** 3874
[12] Lent C S, Sivaprakasam S and Kirkner D J 1989 *Solid State Electron.* **32** 1137
[13] Szafer A and Stone A D 1989 *Phys. Rev. Lett.* **62** 300
[14] Kirczenow G 1988 *Solid State Commun.* **68** 715
[15] Bagwell P F and Orlando T P 1989 *Phys. Rev.* B **40** 1456
[16] Edelstein V M 1990 *Solid State Commun.* **73** 233
[17] Patel N K, Martín-Moreno L, Nicholls J T, Pepper M, Frost J E F, Ritchie D A and Jones G A C 1992 *Superlatt. Microstruct.* at press
[18] Patel N K, Nicholls J T, Martín-Moreno L, Pepper M, Frost J E F, Ritchie D A and Jones G A C 1991 *Phys. Rev.* B **44** 10973
[19] van Wees B J, Kouwenhoven L P, van Houten H, Beenakker C W J, Mooij J E, Foxon C T and Harris J J 1988 *Phys. Rev.* B **38** 8625
[20] Wharam D A, Ekenberg U, Pepper M, Hasko D G, Ahmed H, Frost J E F, Ritchie D A, Peacock D C and Jones G A C 1989 *Phys. Rev.* B **39** 6283
[21] Zagoskin A M 1991 *JETP Lett.* **52** 435 (1990 *Zh. Eksp. Teor. Fiz.* **52** 1043)
[22] Patel N K, Nicholls J T, Martín-Moreno L, Pepper M, Frost J E F, Ritchie D A and Jones G A C 1991 *Phys. Rev.* B **44**
[23] Glazman L I, Lesovik G B, Khmel'nitskii D E and Shekter R I 1988 *JETP Lett.* **48** 239 (1988 *Zh. Eksp. Teor. Fiz.* **48** 218)
[24] Imry Y 1986 *Directions in Condensed Matter* ed G Grinstein and G Mazenko (Singapore: World Scientific)
[25] Büttiker M 1990 *Phys. Rev.* B **41** 7906
[26] Glazman L I and Jonson M 1989 *J. Phys.: Condens. Matter* **1** 5547
[27] Fertig H A and Halperin B I 1987 *Phys. Rev.* B **36** 7969
[28] Duif A M, Jansen A G M and Wyder P 1989 *J. Phys.: Condens. Matter* **1** 3157
[29] Bever T, Wieck A D, Klitzing K von, Ploog K and Wyder P 1991 *Phys. Rev.* B **44** 6507